Recent Developments of Smoothed Particle Galerkin (SPG) Method for Joint Modeling

Youcai Wu, Wei Hu, Xiaofei Pan, C.T. Wu

Livermore Software Technology, an ANSYS company
7374 Las Positas Road, Livermore, CA 94551, U.S.A.

Abstract

This paper presents the most up-to-date status of SPG (Smoothed Particle Galerkin) development with a focus on the establishment of a failure criterion library, a default keyword parameter setting, and its application in joint modeling. In the recent years, SPG bond failure criterion has been extended from effective plastic strain to 1st/3rd principal strain, maximum shear strain, 1st principal stress and several other quantities defined through *MAT_ADD_EROSION (e.g. effective stress/strain and GISSMO damage). Meanwhile, to minimize users' work in setting up an SPG simulation, default parameters have been provided so that user can set up the SPG material failure analysis easily with as few as one prescribed parameter for the failure criterion. To demonstrate the effectiveness of SPG method with the new features, the failure modeling of FDS (flow drill screwing) and spot welding is studied.

Keywords: SPG, failure, joint modeling

Introduction

The SPG method [1, 2], a genuine particle method, exclusively available in LS-DYNA®, was first introduced in 2015. It was particularly developed for modeling ductile material failure. Different from the conventional FEM (finite element method) where element erosion technique is employed to model material separation, which leads to undesired mass, momentum and energy loss, the SPG method utilizes a bond-based failure mechanism to mimic the discontinuity (due to material separation) in displacement field without violating the conservation laws in physics. Furthermore, to improve the efficiency and stability, the SPG weak form is integrated using the direct nodal integration (DNI) technique that is stabilized by a non-residual type stabilization term derived from displacement smoothing. The DNI scheme, without using any background mesh / cell (otherwise impractical to be built once separation occurs), makes SPG method feasible to accurately simulate the material separation. The mathematical and numerical analyses [3, 4] have suggested that the SPG method is stable and convergent in modeling material failure processes.

The SPG method has been successfully applied to the analysis of high velocity impact penetration on concrete [4] and metal [5] targets, metal machining (grinding [3], cutting and friction drilling [6, 7]), compression molding [8] of long fiber reinforced polymer, and mechanical joining [9, 10] of metal workpieces. All these modellings share a common feature, i.e., material failure and separation. To further satisfy users' needs in a wide range of material failure analysis, some new features were developed. These include a failure criterion library and a default keyword parameter setting in LS-DYNA R12.

This paper reviews the theory of the SPG method and describes the new features along with the LS-DYNA keyword. To show the effectiveness of the SPG method, two numerical examples, flow drill screwing (FDS) and resistance spot welding (RSW), are investigated.

Overview of SPG

SPG theory

LS-DYNA is a well-known commercial software used in the automobile industry for crashworthiness analysis where material failure needs to be modeled during the crash simulation. Traditionally, material failure is modeled by element erosion technique in the finite element method (FEM) which usually depends on ad-hoc and problem dependent failure criteria. As such, not only conservation laws are violated, but also the failure pattern (deformed mode) cannot be well-predicted.

To capture the physics in a material failure simulation, first of all conservation laws (mass, momentum and energy) need to be preserved. Secondly, the numerical scheme should be convergent and stable. The SPG method was developed in 2015 [1] to meet the needs for material failure analysis.

The theory of the SPG method has been documented elsewhere [1-4], therefore, only the fundamentals are reviewed hereinafter. The semi-discrete form of equation of motion for the explicit dynamic analysis can be written as:

$$\mathbf{M\ddot{u}} = \mathbf{f}^{ext} - \mathbf{f}^{int} \tag{1}$$

with $\mathbf{M}$ being the lumped mass matrix, $\mathbf{\ddot{u}}$ being the acceleration, $\mathbf{f}^{ext}$ being the external force vector and $\mathbf{f}^{int}$ being the internal force vector, which is calculated by:

$$\mathbf{f}_I^{int} = \int_{\Omega_I} \mathbf{B}_I^T \mathbf{\Xi} d\Omega \tag{2}$$

where $\mathbf{B}$ is the gradient matrix and $\mathbf{\Xi}$ is the stress vector.

Eq.(2) needs to be evaluated at each particle at every time step, which is the most time-consuming part in an explicit dynamic analysis. In particle methods, the direct nodal integration (DNI) scheme is used. However, low energy modes will occur if Eq.(1) is solved simply by the DNI scheme [11]. To resolve this numerical issue of particle method, Wu et al [1] proposed a displacement smoothing technique which is inspired by the strain smoothing technique [12] to stabilize the low energy modes and is defined as:

$$\mathbf{\bar{u}}(\mathbf{x}) \Box \sum_{J=1,NP} \Psi_J^{spg}(\mathbf{x}) \mathbf{d}_J \tag{3}$$

$$\Psi_J^{spg}(\mathbf{x}) \Box \sum_{I=1,NP} \tilde{\Psi}_I^s(\mathbf{x}) \Psi_J^a(\mathbf{x}_I) \tag{4}$$

where $\Psi^{spg}(\mathbf{x})$ is the SPG shape function, NP is the number of particles used in the domain discretization, $\Psi^a(\mathbf{x})$ is the displacement shape function with a compact support a and $\tilde{\Psi}^s(\mathbf{x})$ is the displacement smoothing function with a compact support s. In SPG method, $a = s$ is considered for stabilization. With the smoothed displacement field, the semi-discrete Galerkin weak form can be obtained and given by:

$$\mathbf{M\ddot{d}} = \mathbf{f}^{ext} - \mathbf{f}^{int} - \mathbf{\hat{f}}^{stab} \tag{5}$$

where $\mathbf{\hat{f}}^{stab}$ is the stabilization term, which is integrated by DNI as:

$$\mathbf{\hat{f}}_I^{stab} \overset{DNI}{=} \sum_{N=1,NP} \mathbf{\hat{B}}_I^T(\mathbf{X}_N) \mathbf{\hat{\sigma}}(\mathbf{X}_N) J^0 V_N^0 \tag{6}$$

where J^0 is the determinant of the Jacobian matrix and V_N^0 is the volume of particle N. $\mathbf{\hat{B}}$ is the stabilization gradient matrix, which is composed of $\tilde{\Psi}^s(\mathbf{x})$, $\Psi^a(\mathbf{x})$ and their derivatives, and $\mathbf{\hat{\sigma}}$ is the stabilization stress. The mathematical derivations have been documented elsewhere [1-4] and are omitted here.

With the stabilization term introduced in Eq.(5), the numerical system is stable when integrated by the DNI scheme. It is worthy of pointing out that the calculation of stabilization term in Eq.(6) does not involve any artificial control parameters. Although C^1 approximation (alternative to C^0 in FEM) is used in the SPG method, it still can be coupled with FEM through common nodes, which helps to save computational cost in a large-scale problem where only area of interest is modeled by SPG method.

Bond-based failure mechanism

As mentioned beforehand that preservation of conservation laws is critical in material failure analysis. In contrast to element erosion technique used in FEM, a bond-based failure mechanism is introduced to SPG method to preserve the conservation properties of the particle system in material modeling. In the bond-based failure mechanism, each pair of neighboring SPG particles within the particle support forms a numerical bond, which is like a chemical bond. The bond breaks when user defined failure criteria are satisfied. The quantity for criteria could be effective plastic strain, damage indicator, 1st / 3rd principal strain, maximum shear strain, etc. When bond failure occurs, the interaction between the corresponding two particles is disabled. In other words, for a pair of particles I and J, the SPG shape function in Eq.(4) can be redefined as:

$$\Psi_J^{spg}(\mathbf{x}_I) = \begin{cases} 0 & \text{if } \kappa > \kappa^c \text{ and } \lambda > \lambda^c \\ \sum_{K=1,NP} \tilde{\Psi}_K^s(\mathbf{x}_I) \Psi_J^a(\mathbf{x}_K) & \text{Otherwise} \end{cases} \tag{7}$$

where $\kappa = \left[\kappa(\mathbf{x}_I) + \kappa(\mathbf{x}_J)\right]/2$ is the average of the user defined quantity for bond failure such as effective plastic strain $\bar{\varepsilon}^p$ or material damage at particles I and J and κ^c is its critical value. $\lambda = 1 + \|\mathbf{u}_I - \mathbf{u}_J\|/\|\mathbf{X}_I - \mathbf{X}_J\|$ measures the relative deformation (bond stretch ratio) between particles I and J, where $\mathbf{u}$ is the displacement and $\mathbf{X}$ is the coordinates in un-deformed configuration and λ^c is the critical relative deformation for bond failure.

The bond failure mechanism is schematically illustrated in Figure 1. The support of particle 3 (blue ellipse) covers particles 1~4 (including particle 3 itself), and the support of particle 4 (red ellipse) covers particles 3~6 (including particle 4). Initially, the SPG shape functions satisfy the partition of unity, $\sum_{I=1,4} \Psi_I^{spg}(\mathbf{x}_3) = 1.0$ and $\sum_{I=3,6} \Psi_I^{spg}(\mathbf{x}_4) = 1.0$, which is necessary condition in preserving the rigid body motion. After deformation, assume the failure criteria for bond 3-4 are satisfied and the bond is broken, then particle 4 is removed from the neighbor sorting within the support of particle 3 and vice versa (although, geometrically, their supports might still cover each other). The SPG shape functions will be then reconstructed to satisfy $\sum_{I=1,3} \Psi_I'^{spg}(\mathbf{x}_3) = 1.0$ and $\sum_{I=4,6} \Psi_I'^{spg}(\mathbf{x}_4) = 1.0$.
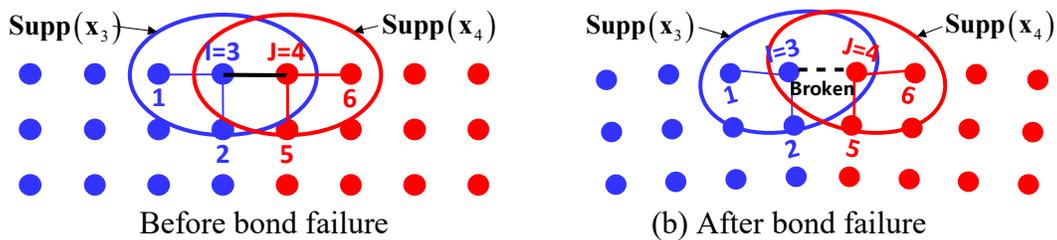
Figure 1. Illustration of SPG bond failure mechanism.

With the new SPG shape functions, the stress and strain at particles 3 and 4 can still evolve independently according to material law. As such, unlike the traditional FEM material failure mechanism, where element is deleted (thus loss of mass, momentum and energy) when failure occurs, the SPG failure mechanism preserves mass, momentum and energy. Table 1 compares the FEM and SPG failure mechanisms. It can be seen that same failure criteria can be used for both approaches, but their outcomes are different as will be shown in the numerical examples.

Table 1 Comparison of FEM and SPG failure mechanisms

	FEM Failure	**SPG Failure**
Criteria	Effective plastic strain Add erosion / GISSMO Mesh dependent	Effective plastic strain Add erosion / GISSMO Less discretization dependence
Upon failure	Set stress to 0: $\Xi = 0$ Element deletion	Regular stress–strain evolution Bond failure without erosion
Conservation	Violated	Conserved
Force	Underestimated	More physical
Failure pattern	Erroneous prediction	Reasonable

LS-DYNA keyword for SPG analysis

It is very simple to set up an SPG simulation in LS-DYNA. The exact same discretization and material laws as for an FEM simulation are used, in which tetrahedron, pentahedron and hexahedron solid elements are also available. The only keyword for activating the SPG formulation is "*SECTION_SOLID_SPG". User only needs to flag a part to this keyword instead of *SECTION_SOLID. An example of SPG keyword cards is shown in Figure 2 with keyword parameters defined in Table 2.

```
*SECTION_SOLID_SPG
$     SECID     ELFORM    NotUsed
          1
$        DX         DY         DZ    ISPLINE     KERNEL    NotUsed     SMSTEP    NotUsed
$      IDAM         FS    STRETCH        ITB                   ISC
                  0.45
```

Figure 2. Parameters on SPG keyword cards.

Table 2 Parameters on SPG control cards

Parameter	Meaning and default
ELFORM	Element formulation, default and the only value is 47
DX, DY, DZ	Normalized support size Default: 1.6 if KERNEL=0 1.8 if KERNEL=1 or ITB=3 1.5 if KERNEL=2
ISPLINE	Kernel function type =0: cubic Spline function (default) =1: quadratic Spline function =2: cubic Spline function with spherical support
KERNEL	Kernel type =0: update Lagrangian, tension dominant problems (default) =1: Eulerian kernel, large and extreme deformation, global response =2: pseudo-Lagrangian kernel, extreme deformation, local response
SMSTEP	Interval of time steps for kernel update Default: 15 if KERNEL=0 5 if KERNEL=1 30 if KERNEL=2
IDAM	Damage indictor (additional see Remark 1) =1: effective plastic strain (default) =2: 1ˢᵗ principal stress =3: maximum shear strain =4: minimum principal strain =5: effective plastic strain + maximum shear strain
FS	Critical value for bond failure of the variable indicated by IDAM
STRETCH	Relative stretching/compression ratio for bond failure Default for mat3, mat24: 1.0+0.4*FS (for elasto-plastic metals) Default for mat72, mat159, mat273: 1.01 (for semi-brittle concrete)
ITB	Stabilization indicator =1: fluid particle (accurate) =2: simplified fluid particle (robust, for high velocity impact problems) =3: momentum consistent smoothing (tension dominant problems) Default: 1 if KERNEL=0 or 1 2 if KERNEL=2
ISC	Indicator for self-contact between failed particles in impact penetration analysis, input Young's modulus of the material to activate it Default: 0, no self-contact (SMP only)

From Figure 2, there are more than 10 parameters on SPG keyword cards to be specified. However, user can also set up an SPG failure analysis at ease by specifying only one parameter for FS, which is used as the bond failure criterion κ^c in Eq.(7) relating to material property, while keep the rest of parameters empty using their default values. The default value of "STRETCH" or λ^c in Eq.(7) is a material dependent parameter.

If "FS" on the material cards of "*MAT_PLASTIC_KINEMATIC" (mat03) or "*MAT_PIECEWISE_LINEAR_PLASTICITY" (mat24) is specified (nonzero), it will overwrite the "FS" on SPG keyword card. Meanwhile, mat03 and mat24, "STRETCH" can be estimated as $1+0.4\kappa^c$. As such, if mat03

or mat24 is used, user can set up an SPG simulation without setting any parameter in the SPG keyword cards. The meaning and default value of each parameter are listed in Table 2.

Besides the variables specified on SPG keyword cards, some quantities defined through *MAT_ADD_EROSION can also be employed as failure criteria. Currently, the following quantities have been adopted as (from highest priority to lowest priority):

    (1) Minimum pressure
    (2) Effective stress (strain rate dependent)
    (3) 1st principal strain (strain rate dependent)
    (4) Maximum pressure
    (5) Effective strain
    (6) Volumetric strain

GISSMO damage has also been implemented as bond failure indicator, which is input through *MAT_ADD_EROSION (IDAM=1) or *MAT_ADD_DAMAGE_GISSMO.

Among all the failure criteria, GISSMO damage has the highest priority, followed by the quantities defined through *MAT_ADD_EROSION, and the variables specified in SPG keyword cards have the lowest priority. If multiple criteria are defined, only the highest priority one will be applied.

Joint performance analysis

To show the effectiveness of SPG method, joint strength analyses are performed in this section. Joints are used in nearly every industry, such as automobile, aerospace, electronics, construction machinery, household appliances, medical device, and shipbuilding. Each joint has a limited strength which depends on the joining material, base material and joining process. Joint strength is a critical factor in design optimization of any structure. Therefore, joint performance is investigated using the SPG method hereafter.

Lap shear of spotweld

RSW (Resistant Spot Welding) is a widely used joining technology in automotive industry for joining steel plates. The performance of RSW joints is crucial to vehicle integrity and occupants' safety. In this section, one of the standard static joint performance tests, i.e., lap shear response of a spotweld is modeled. The spotweld to be modeled has a diameter 6.0 mm fusion zone (FZ, or nugget), 0.5 mm thick ring of heat affected zone (HAZ). The DP980 steel plates to be connected have a thickness of 1.2 mm. The material properties are taken from Ref. [13, 14] and piecewise linear plasticity model is used for its stress – strain evolution. The yield strength for BM (base material), HAZ and FZ is 710 MPa, 584 MPa and 800 MPa respectively. The discretization of the spotweld is shown in Figure 3 (a): (1) the central Ø5.0 mm FZ – FEM, remaining 0.5 mm thick ring of FZ – SPG; (2) HAZ – SPG; (3) 1.0 mm thick ring of BM – SPG, remaining BM – FEM. Common nodes are used between different parts. By doing so, not only SPG zone is minimized and thus reduces computational cost but failure is allowed in all regions. A constant velocity of 5.0 mm/s is applied at both ends of the tension bar (Figure 3 (b)).
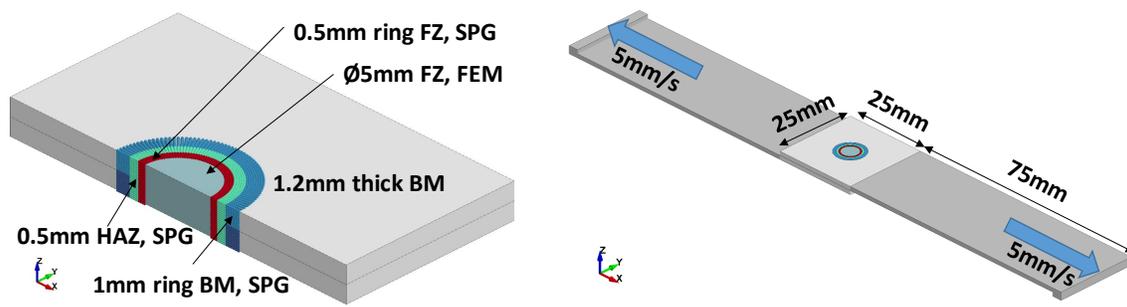
    (a) Section view of a spotweld   (b) Setup of lap shear test

Figure 3. Modeling of spotweld lap shear test.

```
*SECTION_SOLID_SPG
$FZ
$     SECID    ELFORM   NotUsed
          1
$        DX        DY        DZ   ISPLINE    KERNEL   NotUsed    SMSTEP   NotUsed

$      IDAM        FS   STRETCH       ITB                 ISC
          3       0.6
```

Figure 4. SPG setup for spotweld lap shear test.

As shown in Figure 4, default SPG parameters are used except the failure mechanism. Lap shear is a shear dominant process, therefore, maximum shear strain is selected as the bond failure indicator. Considering the differences in microstructures of FZ, HAZ and BM, the critical shear strain ("FS") is set to 0.6, 0.9 and 1.2 respectively for these regions.

(a) Convergence   (b) Sensitivity to failure criteria
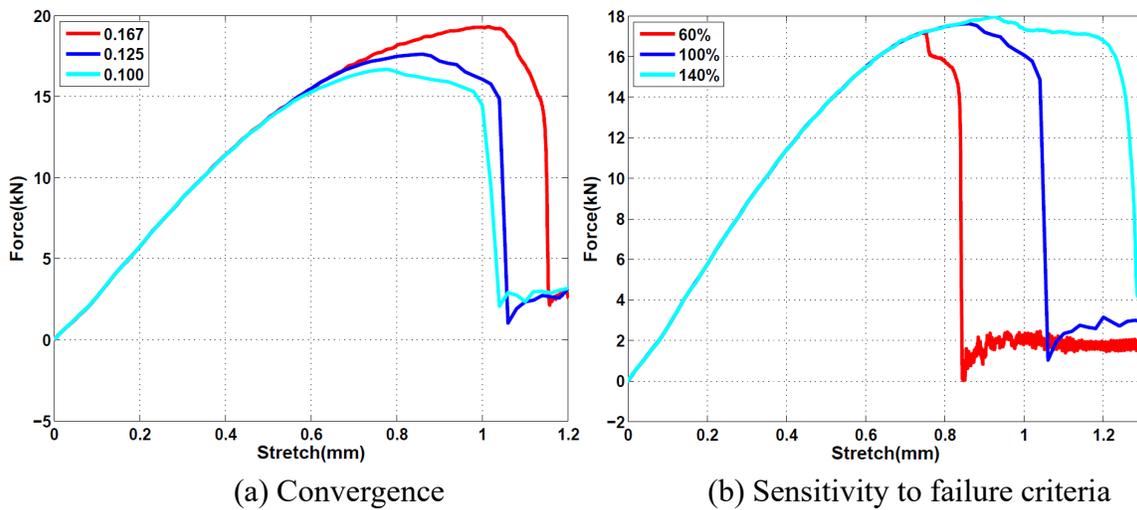
Figure 5. Force responses obtained from SPG simulations.

Figure 5 shows the force responses for various conditions. In Figure 5 (a), different discretizations are used. The legend is the shortest paticle distance in SPG zone. The results imply that SPG solution converges. Figure 5 (b) shows the sensitivity of SPG results to the bond failure criteria. 60% / 140% indicates a reduction / increment of 40% on FS for all the three materials. The lap shear strength does not seem to change too much for a 40% variation of failure criterion. However, the energy absorption varies about 20% from one case to another. Energy dissipation is crucial for occupants' protection in a crashworthiness analysis, therefore, physically predicting joint energy absorption is very important. Figure 6 shows the failure mode of a lap sheared spotweld. Nugget pullout is observed, which is the desired failure mode. Partial HAZ crushing is also observed, which is reasonable since softening occurred during welding process.
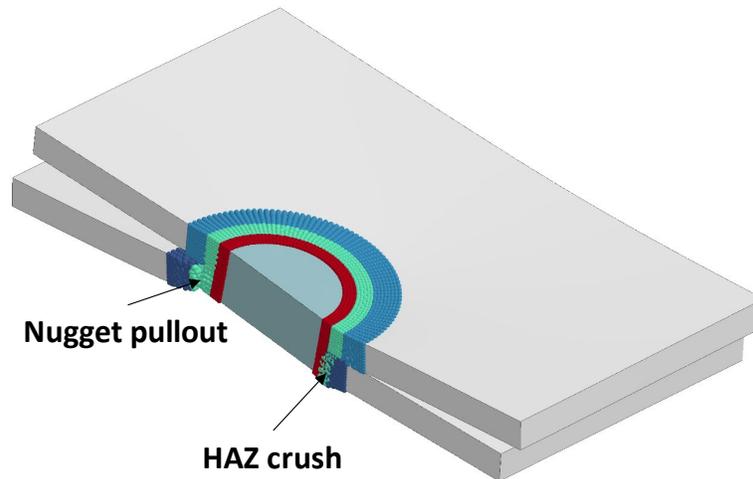
Figure 6. Failure pattern of spotweld lap shear test.

Pullout of flow drill screw (FDS) joint

FDS (Flow Drill Screwing) is a new joining technology emerged along with vehicle weight lightening in automotive industry. The advantages of FDS are one-sided manufacturing and feasibility in joining dissimilar materials. However, material failure occurs during the joining process. To determine the joint's reliability, an FDS joining process is simulated followed by modeling of its pullout strength.
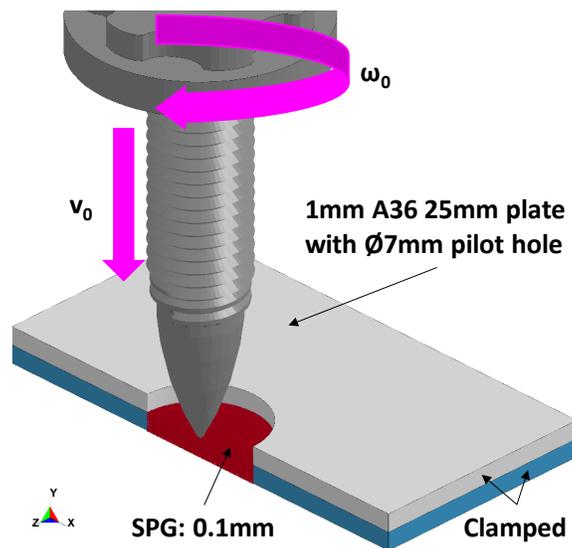
Figure 7. Setup of FDS pullout test.

Figure 7 shows the setup for an FDS joining process followed by pullout test. An M5 screw is used to connect two 1 mm thick ASTM A36 steel plates. The top plate has a diameter 7 mm pilot hole. Once the joining process is completed, a pullout test is performed. All edges of the plates are clamped. The prescribed translational displacement and rotational speed on the screw are shown in Figure 8.

(a) Translational displacement **v₀**   (b) Rotational speed **ω₀**
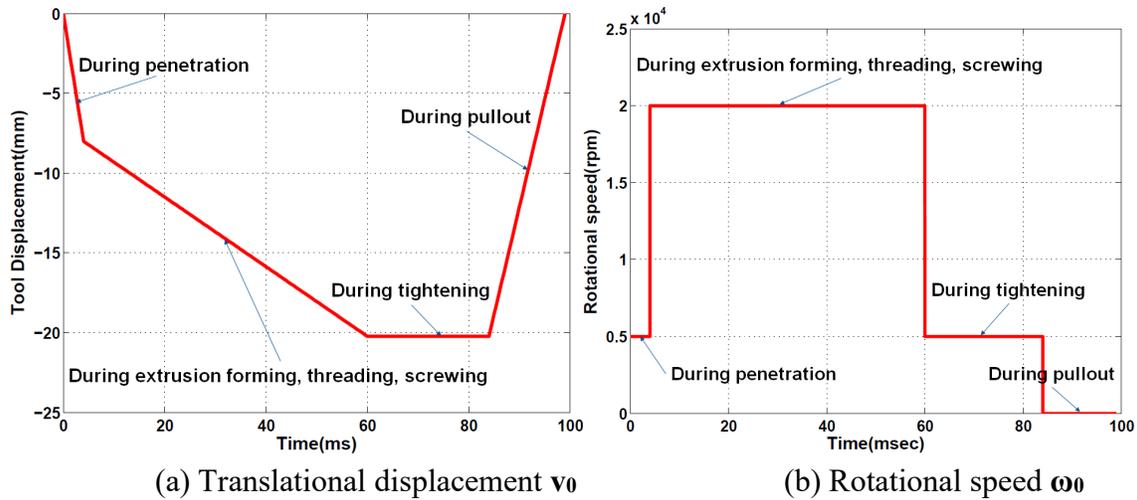
Figure 8. Applied boundary conditions for FDS joining and pullout test.

To save CPU time, only a small region under the pilot hole on the bottom plate is modeled by SPG (c.f. Figure 7) with a shortest particle distance of 0.1 mm. The SPG setup is shown in Figure 9. Default parameters are used except the material dependent failure criteria "FS", which is effective plastic strain at a critical value of 0.5. Johnson-Cook model is employed to describe the constitutive responses of the A36 steel. The screw is assumed to be rigid.

```
*SECTION_SOLID_SPG
$     SECID     ELFORM     NotUsed
          5
$        DX        DY         DZ     ISPLINE    KERNEL    NotUsed    SMSTEP    NotUsed
$      IDAM        FS     STRETCH        ITB                  ISC
                  0.5         1.5
```

Figure 9. SPG setup for FDS joining and pullout test.

Figure 10 shows the deformed shape at different stages. A gap between the plates is observed after screwing (Figure 10 (a)), and closed after tightening (Figure 10(b)), which is physical. Threads on the bottom plate are clearly observed, which means the SPG method captures the most important physics of the FDS joining process, i.e., thread forming. This is on sharp contrast to erosion type failure analysis (FEM).

(a) After screwing   (b) After tightening
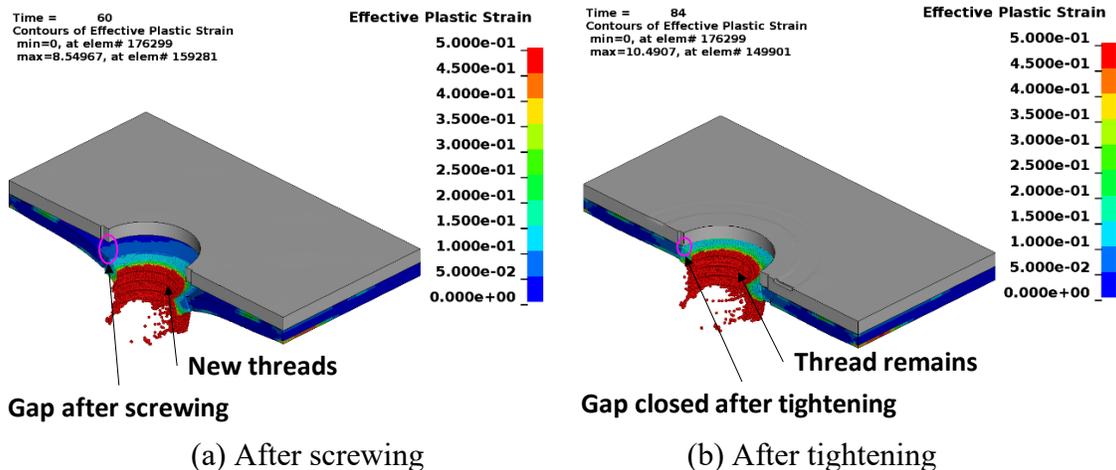
Figure 10. Deformation patterns at different stages in FDS joining process.

Material failure occurred during FDS joining process, thus it is important to check its remaining strength. The force – deflection (both applied on the screw) responses of the FDS joining process and pullout test are plotted in Figure 11. Technically, FDS joining process can be designated into six stages, i.e., heating, penetration, extrusion forming, threading, screwing, and tightening. In this study, heating stage is ignored since only a mechanical analysis is performed. Compressive force is observed during penetration through threading stages. During screwing stage, force changed from compression to tension. This is because some material climbs relatively up along the screw threads. High tension force is built up during tightening stage which tightens and connects the two plates. Finally, even higher tension force is observed during pullout test, which indicates that the joint is effective. The force at each stage is qualitatively consistent with FDS physics.
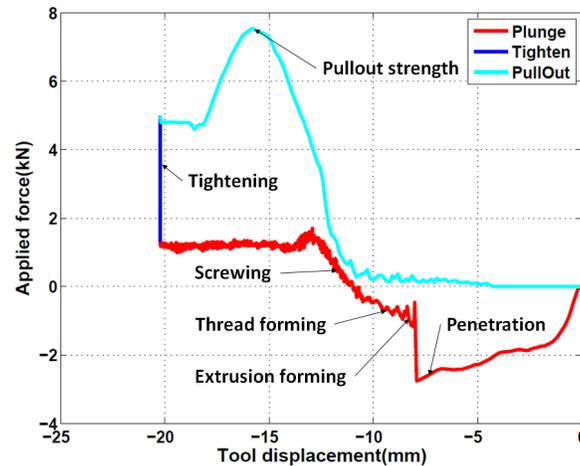
Figure 11. Force – displacement responses for FDS joining and pullout test.

Conclusions

The most up-to-date status of LS-DYNA SPG method is introduced in this paper with focus on bond failure library and default keyword parameter setting. To accommodate more and more applications, SPG bond failure criteria have been expanded to use more state variables and erosion type (*MAT_ADD_EROSION, GISSMO damage) quantities. Furthermore, a set of default keyword parameters was developed so that users can set up an SPG failure analysis with very limited work had they have a model for FEM analysis.

Using nearly the default keyword parameters (except the critical value for SPG bond failure), a spotweld lap shear test was modeled, an FDS joining process was simulated and the FDS joint pullout strength was computed as well. The effectiveness of the SPG method in material failure analysis is demonstrated through the numerical results in that they are qualitatively consistent with physics.

References

1   Wu CT, Koishi M, Hu W. A displacement smoothing induced strain gradient stabilization for the meshfree Galerkin nodal integration method. *Comput. Mech.* **56**, 19-37, 2015.
2   Wu CT, Chi SW, Koishi M, Wu Y. Strain gradient stabilization with dual stress points for the meshfree nodal integration method in inelastic analysis. *Int. J. Numer. Methods Engrg.* **107**, 3-30, 2016.
3   Wu CT, Bui TQ, Wu Y, Luo TL, Wang M, Liao CC, Chen PY, Lai YS. Numerical and experimental validation of a particle Galerkin method for metal grinding simulation. *Comput. Mech.* **61**, 365-383, 2018.
4   Wu CT, Wu Y, Crawford JE, Magallanes JM. Three-dimensional concrete impact and penetration simulations using the smoothed particle Galerkin method. *Int. J. Impact Engrg.* **106**, 1-17, 2017.
5   Wu Y, Wu CT. Simulation of Impact Penetration and Perforation of Metal Targets Using the Smoothed Particle Galerkin Method. *Journal of Engineering Mechanics*, 144(8), 04018057, 2018.

6   Wu CT, Wu Y, Liu Z, Wang D. A stable and convergent Lagrangian particle method with multiple nodal stress points for large strain and material failure analyses in manufacturing processes. *Finite Elements in Analysis and Design*, 146, 96-106, 2018.

7   Pan X, Wu CT, Hu W, Wu Y. A momentum-consistent stabilization algorithm for Lagrangian particle methods in the thermo-mechanical friction drilling analysis. *Comput. Mech.* 64, 625–644, 2019.

8   Hayashi S, Wu CT, Hu W, Wu Y, Pan X, Chen H. New Methods for Compression Molding Simulation and Component Strength Validation for Long Carbon Fiber Reinforced Thermoplastics. *12th European LS-DYNA Conference*, Koblenz, Germany, May 2019.

9   Huang L, Wu Y, Huff G, Huang S, Ilinich A, Freis A, Luchey G. Simulation of Self-Piercing Rivet Insertion Using Smoothed Particle Galerkin Method. *15th International LS-DYNA Users Conference*, Detroit, MI, June, 2018

10 Wu CT, Wu Y, Lyu D, Pan X, Hu W. The momentum-consistent smoothed particle Galerkin (MC-SPG) method for simulating the extreme thread forming in the flow drill screw-driving process. *Comp. Part. Mech.,* doi:10.1007/s40571-019-00235-2, 2019.

11 Belytschko T, Guo Y, Liu WK, Xiao SP. A unified stability analysis of meshless particle methods. *Int. J. Numer. Methods Engrg.* 48:1359-1400, 2000

12 Chen JS, Wu CT, Yoon S, You Y. A Stabilized Conforming Nodal Integration for Galerkin Meshfree Methods. *Int. J. Numer. Methods Engrg.* **50**: 435-466, 2001.

13 Rezayat H, Ghassemi-Armaki H, Bhat SP, Sriram S, Babu SS. Constitutive properties and plastic instabilities in the heat-affected zones of advanced high-strength steel spot welds. *J. Mater. Sci.* 54: 5825-5843, 2019.

14 Park N, Park M, Kwon J, Huh H. Material properties of the nugget zone in resistance spot-welded DP980 steel joint at various strain rates. *Sci. Technol. Weld. Join*. 23: 7-12, 2018.